**The EMBO Journal (2005) 24,** 1537–1545 | © 2005 European Molecular Biology Organization | All Rights Reserved 0261-4189/05
www.embojournal.org

THE EMBO JOURNAL

# Role of curvature and phase transition in lipid sorting and fission of membrane tubules

**Aurélien Roux[1,2,4], Damien Cuvelier[2], Pierre Nassoy[2], Jacques Prost[2,3], Patricia Bassereau[2,5] and Bruno Goud[1,5,*]**

[1]UMR 144 CNRS/Institut Curie, Paris, France, [2]UMR 168 CNRS/Institut Curie, Paris, France and [3]ESPCI, Paris, France

**We have recently developed a minimal system for generating long tubular nanostructures that resemble tubes observed *in vivo* with biological membranes. Here, we studied membrane tube pulling in ternary mixtures of sphingomyelin, phosphatidylcholine and cholesterol. Two salient results emerged: the lipid composition is significantly different in the tubes and in the vesicles; tube fission is observed when phase separation is generated in the tubes. This shows that lipid sorting may depend critically on both membrane curvature and phase separation. Phase separation also appears to be important for membrane fission in tubes pulled out of giant liposomes or purified Golgi membranes.**

*The EMBO Journal* (2005) **24,** 1537–1545. doi:10.1038/sj.emboj.7600631; Published online 24 March 2005
*Subject Categories*: membranes & transport
*Keywords*: lipid sorting; membrane curvature; membrane fission; membrane tubules; phase separation

## Introduction

Similar to proteins, most membrane lipids are transported by vesicular carriers that bud off from one compartment and fuse to another along the secretory and endocytic pathways (van Meer and Lisman, 2002). During budding, sorting occurs, some lipids being incorporated into transport intermediates while others are being excluded (Brugger *et al*, 2000; van Meer and Lisman, 2002). *In vitro* experiments using dioleylphosphatidylcholine (DOPC), cholesterol (Chol) and sphingomyelin (SM) reveal under appropriate conditions the coexistence of two types of fluid membrane organization called liquid-ordered $L_o$ and liquid-disordered $L_d$ phases (Dietrich *et al*, 2001). The composition of $L_o$ and $L_d$ phases is different: compared to the global average composition, $L_o$ is enriched in SM whereas $L_d$ is enriched in DOPC (Edidin, 2003). Thus, the ability of $L_o$ versus $L_d$ phases to bud could be a critical parameter in sorting; transport intermediates may form from a pre-existing lipid domain on the donor membrane (van Meer and Lisman, 2002). This possibility adds up to two already proposed mechanisms: sorting according to molecular shape (Mukherjee *et al*, 1999) and dynamical sorting (Mukherjee and Maxfield, 2000). Depending on their physical state ($L_o$ versus $L_d$), membranes display different capabilities to curve. As a result, domains coexisting on the same vesicle exhibit different curvatures (Julicher and Lipowsky, 1993; Baumgart *et al*, 2003). Conversely, membrane curvature is expected to induce phase separation in multicomponent membranes (Leibler and Andelman, 1987; Seifert, 1993). Another important event in transport is fission of transport intermediates from donor membranes. Evidence exists that fission is directly linked to changes in composition of the lipid bilayer, suggesting that the physical properties of lipids play a direct role in the fission process (Schmidt *et al*, 1999; Huttner and Schmidt, 2000).

We have recently developed an experimental system that allows the formation of very thin membrane tubes with a diameter of several tens of nanometers. Such tubes are pulled from giant unilamellar vesicles (GUVs) made of either controlled phospholipidic membrane or of biological membranes, by the action of molecular motors (kinesins) moving along microtubules (Roux *et al*, 2002). This assay makes the comparison with *in vivo* trafficking events reliable, as the tubes generated have dimensions in the physiological range of sizes of transport intermediates, much smaller than the few micron size buds obtained in some cases with giant vesicles (Baumgart *et al*, 2003). Here, we used this assay to test the ability of $L_o$ and $L_d$ phases to form membrane tubes and to investigate the dynamic sorting of lipids during tube formation and the stability of tubes upon phase separation.

## Results and discussion

### *Phase diagram of brain sphingomyelin/cholesterol/dioleylphosphatidylcholine vesicles*

GUVs were prepared from mixtures of brain sphingomyelin (BSM), Chol and DOPC; they were fluorescently labeled by incorporation of a fluorescent lipid $BODIPY_{FL}$-$C_5$-hexadecanoyl phosphatidylcholine ($BODIPY_{FL}$-$C_5$-HPC) at a concentration of 0.5% mol/mol. A total of 11 different compositions of BSM:Chol:DOPC mixtures were tested for the preparation of GUVs. As shown in Supplementary Figure S1A (Supplementary data), the vesicles displayed domains of different phases corresponding to segregation of lipids to various degrees depending on the relative ratio of BSM, Chol and DOPC. Vesicles with a homogeneous fluorescence, reflecting an absence of lipid segregation, were observed at molar ratios of 1:1:0, 0:1:1, 1:2:1 and 1:2:3 of BSM:Chol:DOPC, respectively. These values correspond to 'high' Chol content (over 30%). Vesicles with both highly and weakly fluorescent domains of various sizes were observed at lower Chol concentrations (molar ratios of 3:2:1 and 3:1:3). In the absence of Chol, at molar ratios of 3:0:1, 1:0:1 and 1:0:3,

*Corresponding author. UMR 144 CNRS/Institut Curie, 26 rue d'Ulm, 75248 Paris Cedex 05, France. Tel.: +33 1 4234 6398; Fax: +33 1 4234 6382; E-mail: bruno.goud@curie.fr
[4]Present address: Yale School of Medicine, Boyer Center for Molecular Medicine, 295 Congress Avenue, New Haven, CT 06510, USA
[5]These authors contributed equally to this work

**Received: 17 January 2005; accepted: 25 February 2005; published online: 24 March 2005**

coexistence between a solid-ordered phase and an $L_d$ phase was observed, as previously reported (de Almeida *et al*, 2003).

The ganglioside GM1 is known to specifically segregate into the $L_o$ phase enriched in SM (Dietrich *et al*, 2001). As shown in Figure 1A, BODIPY$_{FL}$-C$_5$-HPC and GM1 stained with fluorescent cholera toxin (which specifically binds to GM1) did not overlap in a segregated vesicle (3:1:3). This observation shows that BODIPY$_{FL}$-C$_5$-HPC was segregated into the $L_d$ phase. The fluorescence ratio of BODIPY$_{FL}$-C$_5$-HPC between fluorescent and nonfluorescent phases on equatorial confocal planes of vesicles of various lipid compositions was found to decrease upon increase of Chol concentration (Supplementary Figure S1B). This observation is compatible with the fact that Chol favors lipid mixing. In agreement with previous reports (Veatch and Keller, 2002; Kahya *et al*, 2003), the Chol concentration thus appeared critical for the formation of lipid domains. We then constructed a schematic phase diagram from our data (Figure 1B and Table I). The gray area corresponds to lipid compositions for which the GUVs exhibit phase separation. The 1:1:1 vesicles represent a frontier situation in which lipids can be segregated or not depending on small changes in Chol concentration. This phase diagram is in good agreement with results obtained with various techniques (de Almeida *et al*, 2003; Kahya *et al*, 2003; Lawrence *et al*, 2003; Veatch and Keller, 2003).

### *Induction of phase separation*

GUVs made of the 1:1:1 lipid mixture showed particular properties. The majority exhibited a uniform fluorescence phase. Without excluding the possibility that small nanodomains of $L_o$ phase, below the optical resolution, exist (Lawrence *et al*, 2003), this suggests that lipids are in one phase ($L_d$) on these GUVs. However, the others (10–30% of the population) showed a fluorescent domain covering only one hemisphere (Supplementary Figure S1A). Interestingly, fluorescence excitation of homogeneous vesicles led to the progressive appearance of small nonfluorescent domains that rapidly fused together (Figure 1C and Supplementary Figure S1A). Similar observations were made with 3:4:1 mixtures (data not shown). As the kinetics of domain formation was dependent on light intensity, two conditions (described in Materials and methods) were used to generate domains, one leading to domain appearance within 1 s ('strong' induction) and the other within 10 s ('weak' induction). Homogeneous vesicles of other lipid compositions did not form domains under the same conditions, as shown in Figure 1C, for a 0:1:1 mixture. This suggests that for compositions very close to the phase transition (such as 1:1:1 and 3:4:1 lipid mixtures), very small changes in lipid concentration can induce phase separation. Indeed, photoactivation of 1:1:1 vesicles generated small amount of oxidized Chol, as shown by thin-layer chromatography (TLC; Supplementary Figure S2A and Supplementary data). About 10 times more oxidized Chol was generated after strong induction as compared to weak induction (Supplementary Figure S2C). In addition, incorporation of Chol (6% n/n) to photoactivated lipid mixtures led to the formation of homogeneous GUVs, which were again sensitive to photoactivation (Supplementary Figure S2B).

The above results suggest that photoactivation causes the depletion of Chol, and that a small decrease in the Chol content of 1:1:1 GUVs is sufficient to promote phase separation. To test this hypothesis directly, 1:1:1 GUVs were incubated with the Chol-sequestering agent methyl-β-cyclodextrin (MβCD) (Kilsdonk *et al*, 1995). As illustrated in

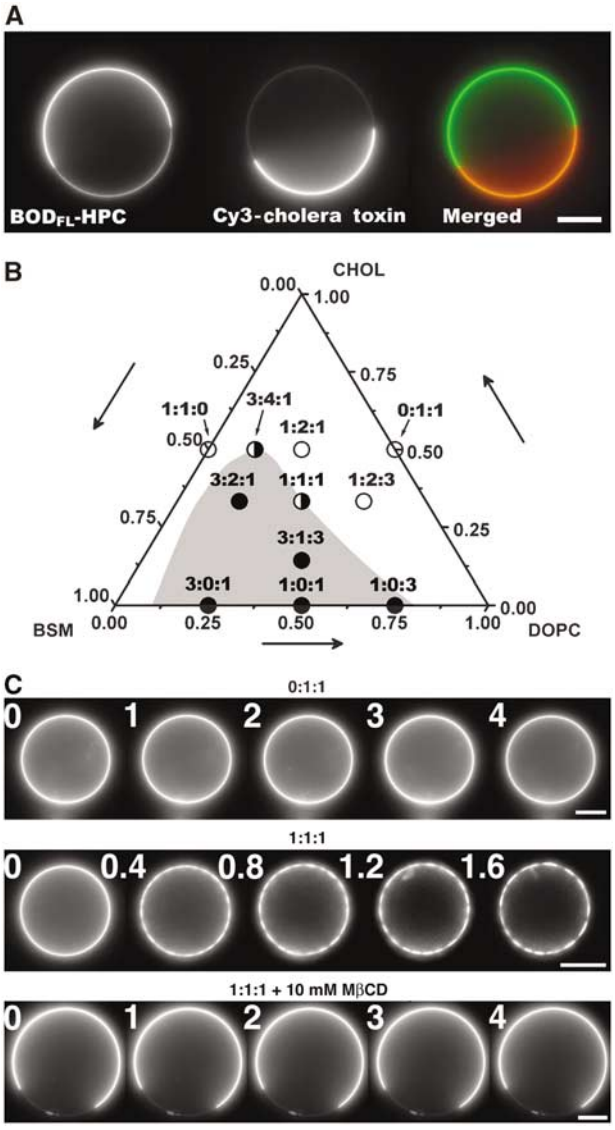


**Figure 1** Phase separation in GUVs. (**A**) Segregation of BODIPY$_{FL}$-C$_5$-HPC and GM1-ganglioside in a 3:1:3 GUV. GM1 was labeled by addition of 3 μg/ml of Cy3-cholera toxin in the buffer. Left image: BODIPY$_{FL}$-C$_5$-HPC partially segregates between the two domains; middle image: GM1 is only present in the $L_o$ domain; right: note the perfect complementarity of the domains. Bar, 10 μm. (**B**) Schematic phase diagram deduced from data obtained with 11 different compositions of lipid mixture at room temperature (22°C). The gray area represents the predicted region where vesicles show domains without photoactivation or treatment with MβCD. The white area corresponds to homogeneous vesicles. Filled circles: compositions showing phase separation; open circles: compositions that are homogeneous and not sensitive to photoactivation; half-white, half-filled circles: compositions at the frontier between segregated and nonsegregated states. (**C**) Induction of phase separation of lipids by strong photoactivation. Vesicles made of only DOPC and Chol (0:1:1) do not exhibit formation of domains under photoactivation. In contrast, photoactivation of GUVs made of BSM, Chol and DOPC (1:1:1) induces the apparition of small domains that rapidly fuse together. Photoactivation had no effect when lipids were segregated by incubation of GUVs in the presence of 10 mM MβCD. Time is in seconds. Bars, 10 μm.

**Table I** Summary of the effects of photoactivation on phase separation and tube fission for different compositions

| Composition BSM:Chol:DOPC | State | Phase separation induced by light | Phase separation induced by MβCD | % Tubes connected to fluorescent phase | % Fission under strong illumination | % Fission under weak illumination |
|---|---|---|---|---|---|---|
| 0:1:1 | NS | No | No | — | 0 | 0 |
| 1:1:0 | NS | No | No | — | 0 | 0 |
| 1:2:3 | NS | No | No | — | 0 | 0 |
| 1:2:1 | NS | No | Yes | — | 0 | 0 |
| 1:1:1 | NS/S | Yes | Yes | Seg 100 | 88 | 0 |
| 3:4:1 | NS/S | Yes | Yes | — | 87 | 0 |
| 3:2:1 | S | No | ND | 57.7 | 0 | 0 |
| 3:1:3 | S | No | ND | 100 | 0 | 0 |

NS: nonsegregated; S: segregated; ND: not determined. The measurement of the % tubes connected to the fluorescent phase is nonrelevant for homogeneous vesicles.

Figure 1C, 10 mM MβCD induced the appearance of domains on all homogeneous 1:1:1 vesicles. Additionally, MβCD did not induce phase separation on homogeneous vesicles of other lipid compositions (1:1:0, 0:1:1 and 1:2:3), except for the 1:2:1 mixture (data not shown). Most likely, MβCD removes more Chol from membranes than photoactivation (about 20%, as estimated using the phase diagram described above), explaining why 1:2:1 vesicles do not form domains upon photoactivation (data not shown).

### *Two different mechanisms for lipid sorting*

Membrane tubes were then pulled out of GUVs prepared from various lipid mixtures. The force $f$ required to pull tubes is proportional to the square root of the bending rigidity $\kappa$ and of the membrane tension $\sigma$: $f = 2\pi\sqrt{2\kappa\sigma}$ (Derenyi *et al*, 2002). Of note, this equation neglects the contribution of the nonlocal bending rigidity, which is due to the difference between inner and outer leaflet areas. Indeed, this effect becomes significant only for tubes longer than several hundreds of microns and at a time scale of the order of 1 min (Svetina *et al*, 1998), which is not the case under our experimental conditions. To our knowledge, no direct measurement of the bending rigidity of SM-rich $L_o$ phases has been reported so far. The measurement of the force $f$ at fixed tension was obtained using an optical tweezers setup coupled to a micropipette system (see Materials and methods and Figure 2). The force was measured at different tensions for the 1:1:0 (Figure 2) and 0:1:1 compositions. For instance, at $\sigma = 5 \times 10^{-5}$ N/m, values of $36 \pm 5$ and $21 \pm 5$ pN were measured for 1:1:0 and 0:1:1 vesicles, respectively. From the plot of force $f$ versus $\sqrt{\sigma}$, we deduced the corresponding bending rigidities: $31 \pm 2 \times 10^{-20}$ J ($65 \pm 6$ kT) and $12 \pm 1.2 \times 10^{-20}$ J ($30 \pm 3$ kT) for 1:1:0 and 0:1:1 compositions, respectively (Figure 3A). Thus, 1:1:0 membranes ($L_o$ phase) are about 2.2 times more rigid than 0:1:1 membranes ($L_d$ phase), in relative good agreement with the values deduced from the shape analysis of buds in segregated vesicles (Baumgart *et al*, 2003). Consequently, for the same tension, the radius of 0:1:1 tubes ($L_d$ phase) should be about 1.5 times smaller than that of 1:1:0 tubes ($L_o$ phase), as $R = \sqrt{\kappa/2\sigma}$ (Derenyi *et al*, 2002). Note that for $\sigma = 5 \times 10^{-5}$ N/m, the diameters of the tube in $L_d$ and $L_o$ phases are expected to be equal to 70 and 110 nm, respectively. However, these values are below the optical resolution and cannot be measured accurately with our optical tweezers setup under controlled membrane tension.

From the above data, we expected that molecular motors should preferentially pull tubes out of the $L_d$ phase in

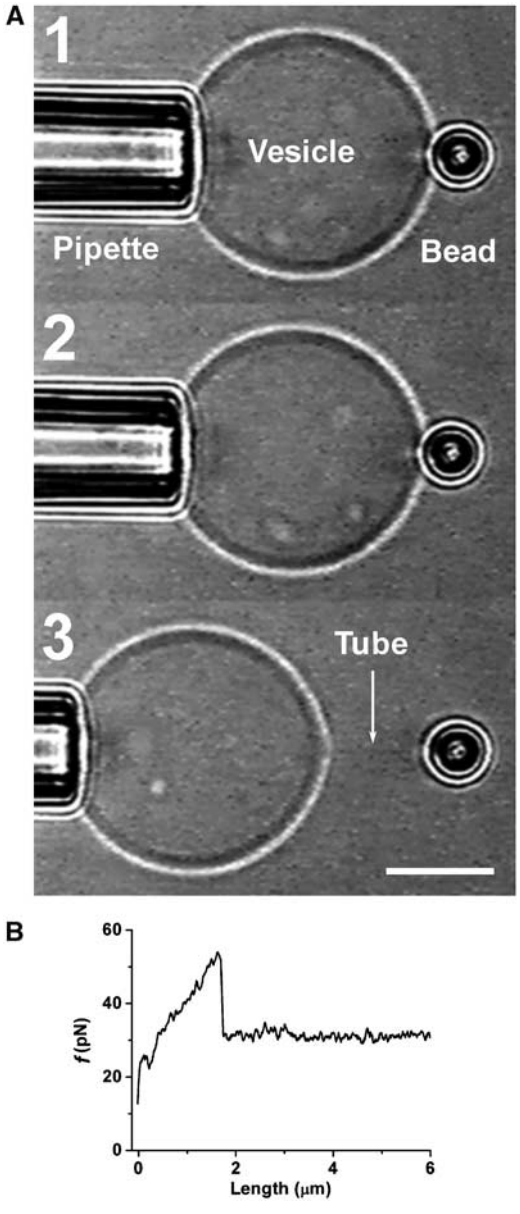


**Figure 2** Measurement of GUV bending rigidity using a micropipette and optical tweezers. (**A**) (1) A GUV aspirated into a micropipette has a fixed tension. (2) The GUV containing biotinylated lipids is pressed against a 3.5 μm diameter streptavidin bead trapped by the optical tweezers. (3) The GUV is retracted and a thin tube can be formed. Bar, 10 μm. (**B**) A typical force–tube extension curve obtained for a 1:1:0 vesicle at a fixed tension ($\sigma = 1.3 \times 10^{-5}$ N/m) during the tube extraction.

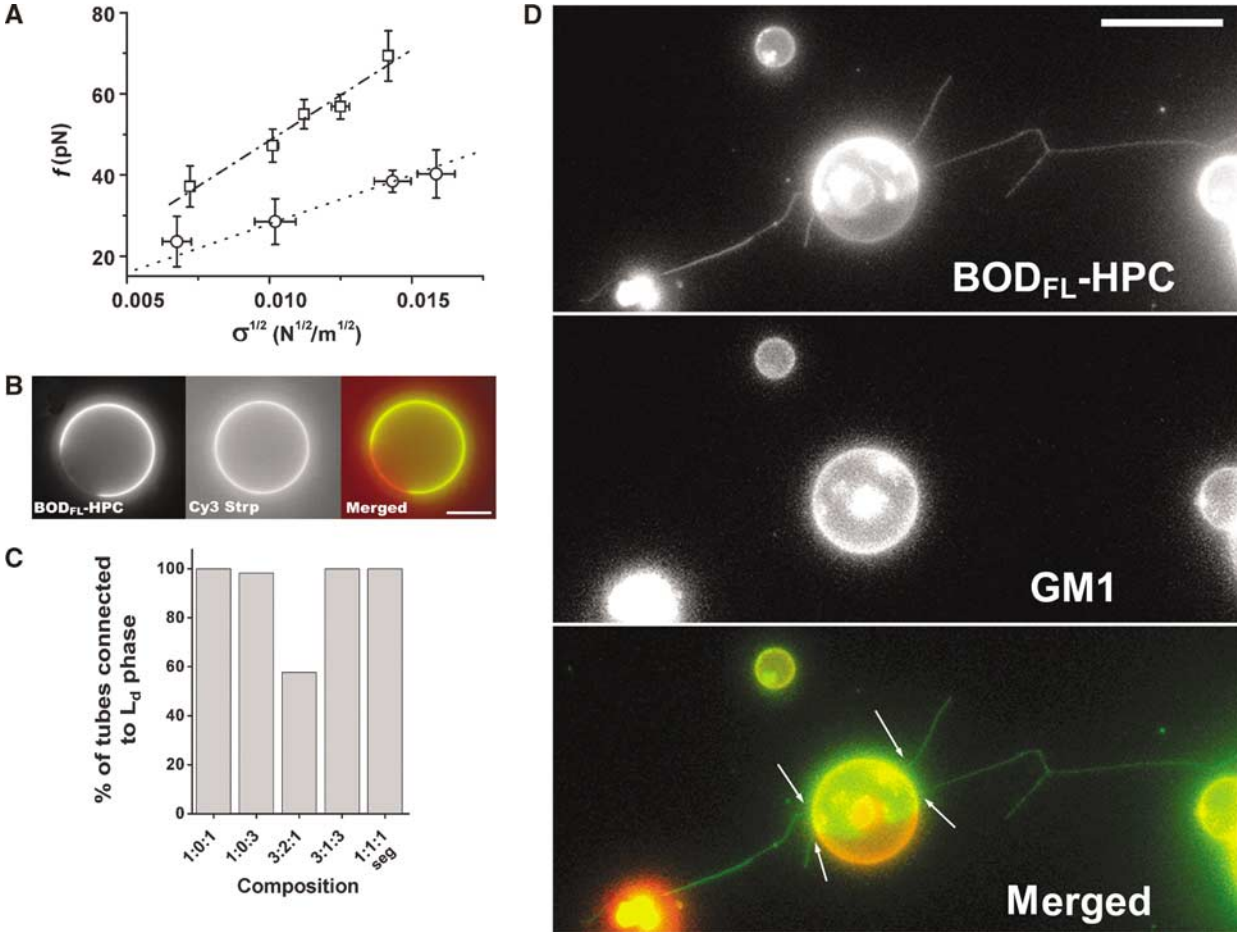


**Figure 3** Lipid sorting in tubes pulled out of 'segregated' vesicles. (**A**) Linear variation of the force *f* required to extend a tube from a vesicle in the $L_o$ phase (1:1:0) (squares) and in the $L_d$ phase (0:1:1) (circles) as a function of the square root of the membrane tension $\sqrt{\sigma}$. The experiments were performed on seven (squares) and 11 (circles) vesicles, as described in the text. Line slopes are proportional to the square root of the bending rigidities $\sqrt{\kappa}$. (**B**) Segregation of fluorescent and biotinylated lipids in a vesicle (3:1:3 mixture): $BODIPY_{FL}$-$C_5$-HPC ($BOD_{FL}$-HPC) is segregating in the $L_d$ phase; note in the middle image that the biotinylated Cap-DOPE labeled with Cy3-streptavidin (Cy3 Strp) is not segregated. Bar, 10 μm. (**C**) Percentage of tubes connected to the $L_d$ phase labeled with $BODIPY_{FL}$-$C_5$-HPC versus lipid composition: 1:1:1 seg is the segregated subpopulation of 1:1:1 GUVs (see Supplementary Figure S1A). For each lipid composition, between 60 and 120 tubes were examined. (**D**) Tubes pulled out of a 'segregated' vesicle (3:1:3 mixture) labeled with both $BODIPY_{FL}$-$C_5$-HPC ($BOD_{FL}$-HPC) (green) and fluorescent cholera toxin-GM1 complex (red). Tubes appear green and connected to the green domain (arrows). They are thus in the $L_d$ phase. White fluorescent spots are bead aggregates, which do not interfere with the experiment. Bar, 10 μm.

segregated vesicles since the force required is lower. This was experimentally verified in our assay upon observation of tubes pulled by kinesins using fast 3D video microscopy (Savino *et al*, 2001). Biotinylated lipid used to anchor kinesins to membrane being equally distributed within the $L_d$ and $L_o$ phases (illustrated in Figure 3B for 3:1:3 GUVs), motors are able to pull on both phases. However, in segregated vesicles labeled with $BODIPY_{FL}$-$C_5$-HPC, the majority of the tubes were not only fluorescent but also connected to the fluorescent domains (Figure 3C). This suggests that tubes were essentially composed of membranes in $L_d$ phase enriched in DOPC. We further checked that GM1, which segregates specifically into the $L_o$ phase, was indeed essentially excluded from tubes (Figure 3D). For 3:1:3, 1:0:3, 1:0:1 and the segregated subpopulation of 1:1:1, 90–100% of the tubes were in the $L_d$ phase. Even in the case of 3:2:1 mixture, which led to a high proportion of $L_o$ phase (between 2/3 and 3/4; see Supplementary Figure S1), this proportion was still of the order of 50% (Figure 3C). Taken together, these data indicate that the bending rigidity of the $L_o$ phase does not favor the formation of highly curved structures in the diameter range of physiological transport intermediates such as endosomal and Golgi tubules. Thus, differences in the ability of phases to form curved structures can lead to lipid sorting.

Importantly, sorting between fluorescent lipids used as markers also occurred in tubes grown from nonsegregated vesicles. Direct evidence came from the comparison of GM1 (labeled by Cy3-cholera toxin) and $BODIPY_{FL}$-$C_5$-HPC amounts present in tubes and in vesicles, as shown in Figures 4A and B. Tubes were pulled out of homogeneous 1:1:1 vesicles containing 1% GM1 (labeled by Cy3-cholera toxin) and 0.5% $BODIPY_{FL}$-$C_5$-HPC. The fluorescence ratio between $BODIPY_{FL}$-$C_5$-HPC and GM1 was increased in the tube as compared to the donor vesicle (Figure 4B). Even though important *per se*, this result could very well concern the fluorescent lipids only. The following observation shows that this is more general and concerns the nonfluorescent lipids as well. We pulled tubes out of homogeneous vesicles

 

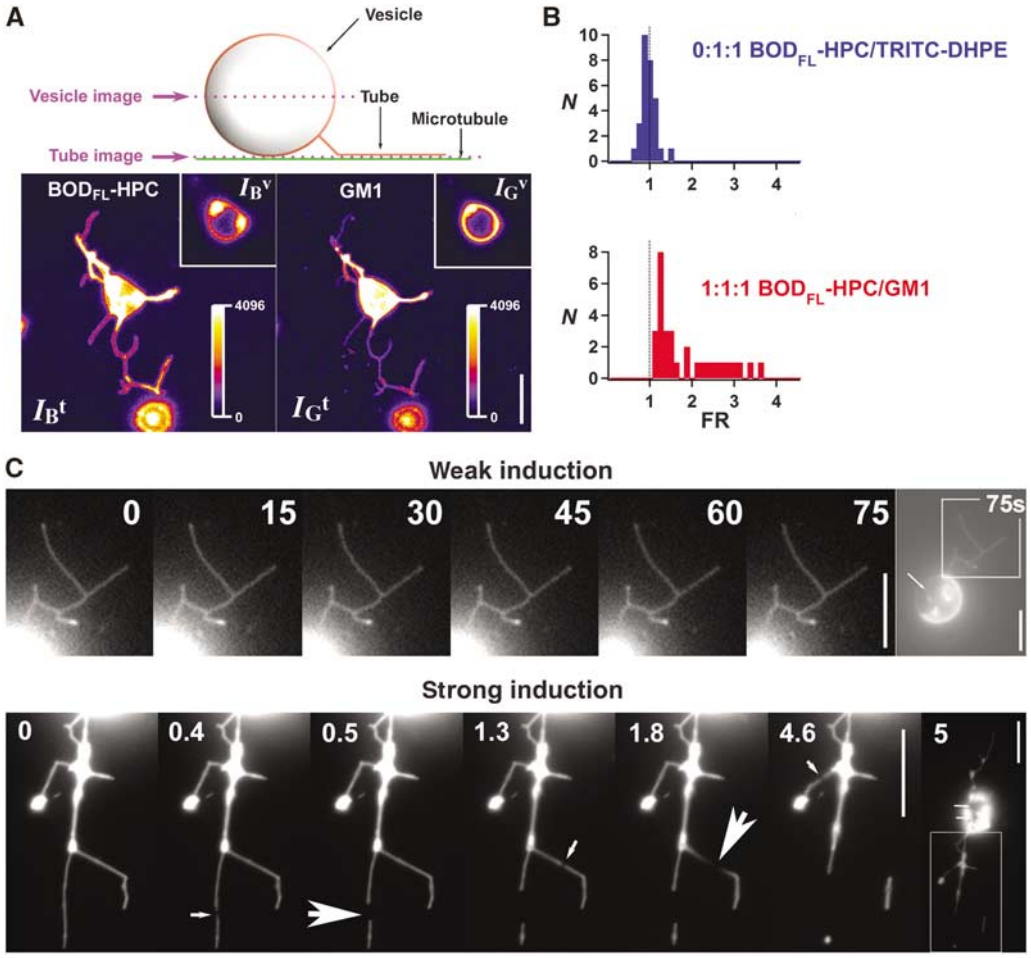


**Figure 4** Lipid sorting in tubes pulled out of homogeneous vesicles (1:1:1 mixture). (**A**) Confocal images of tubes pulled out of membranes labeled with BODIPY$_{FL}$-C$_5$-HPC lipids (BOD$_{FL}$-HPC) and Cy3-cholera toxin–GM1 complexes (GM1). Images were recorded at two levels: one at the vesicle equator (vesicle image) and one on the substrate (tube image) (for more details, see Supplementary data). Left fluorescence image corresponds to the BOD$_{FL}$-HPC channel, whereas the right image to the GM1 channel. Tube images show that the (BOD$_{FL}$-HPC) intensity is higher than that of Cy3-cholera toxin (GM1), whereas it is the opposite in the vesicle image (see insets). Fluorescence intensities of BOD$_{FL}$-HPC and GM1 respectively in the tubes ($I_B^t$, $I_G^t$) and in the vesicle ($I_B^v$, $I_G^v$) were measured from tube and vesicle images (see Materials and methods). Highly fluorescent dots on the vesicle images correspond to the connection between the tubes and the vesicle. Bar, 10 μm. (**B**) The fluorescence ratio FR = $(I_B^t/I_G^t)/(I_B^v/I_G^v)$ was calculated for each network. Two compositions were tested: 0:1:1 and 1:1:1. For 0:1:1 ($L_d$ phase), the vesicles contained two $L_d$ phase fluorophores (BOD$_{FL}$-HPC and TRITC-DHPE) as a control experiment; the FR histogram (blue) calculated from 30 different networks was centered on the value 1, indicating that no relative sorting occurs under these conditions. For 1:1:1, vesicles contained 1% GM1 and 0.5% BOD$_{FL}$-HPC; FR histogram (red) shows that values obtained from 30 different networks were always superior to 1, reflecting a relative depletion of GM1 in tubes or equivalently a relative enrichment in BOD$_{FL}$-HPC. (**C**) Tubes pulled out of homogeneous vesicles (1:1:1 mixture) during phase separation by weak and strong photoactivation. Under weak photoactivation, no phase separation is observable along the tubes even after 75 s of constant illumination, whereas the vesicle has reached a complete segregation (the arrow points to the $L_o$ domain). Under strong photoactivation, very small weakly fluorescent domains appear on tubes (see medium size arrows), leading to fission (big arrows). The vesicle is segregated after 5 s of constant illumination (small arrows point to $L_o$ domains). The enlarged area showing tubes is delimited in the last picture. Note the downscaling of the fluorescence intensities in the tubes compared to those present in the vesicles, due to the small number of fluorescent molecules in a nanometer size tube. Bars, 10 μm.

made of 1:1:1 mixtures. If no lipid sorting was at work, subsequent photoactivation should trigger phase separation in the tubes at lower intensities than in the vesicle. Indeed, in a tube, the phase separation instability is more easily attained due to its coupling to the pearling instability (Derenyi *et al*, 2004). This was not the case. Under weak illumination, the vesicles showed phase separation whereas tubes did not (Figure 4C). Only under strong illumination did the tube show phase separation visualized by the appearance of small weakly fluorescent domains (Figure 4C). This event led to tube fission as described in the next section. This shows that the lipid composition was not the same in the tube and in the vesicle. The further observation that with BODIPY$_{FL}$-C$_5$-HPC labeling, the nonfluorescent phase represented only about 10% of the tube area as compared to 50% in the GUV (Figure 4C) shows that sorting was efficient. Since the nonfluorescent $L_o$ phase is richer in Chol and BSM than the fluorescent $L_d$ phases (de Almeida *et al*, 2003), this observation implies that tubes are depleted of both Chol and BSM. We have thus evidenced that sorting of lipids in tubes can be achieved in two ways: in the first way, phase separation has already occurred on the vesicle and tubes are enriched in lipids of one phase; in the second way, lipids are initially mixed in the membrane and are subsequently sorted upon tube formation on the basis of their molecular properties. This second mechanism is due to the change in bending

modulus with lipid relative proportions (Seifert, 1993; Derenyi *et al*, 2004). It is important to note that because both ways of sorting are only dependent on differences in the bending rigidities of different lipid compositions, they both depend on membrane curvature of the studied structures, and thus on their size. We show here that in the range of sizes of intracellular transport intermediates (tens of nm), these two ways of lipid sorting occur, and thus are likely to take place in cells.

### *Phase separation induces membrane fission*

We have furthermore observed that the induction of phase separation on tubes pulled out of 1:1:1 and 3:4:1 homogeneous GUVs provoked numerous fission events (Figures

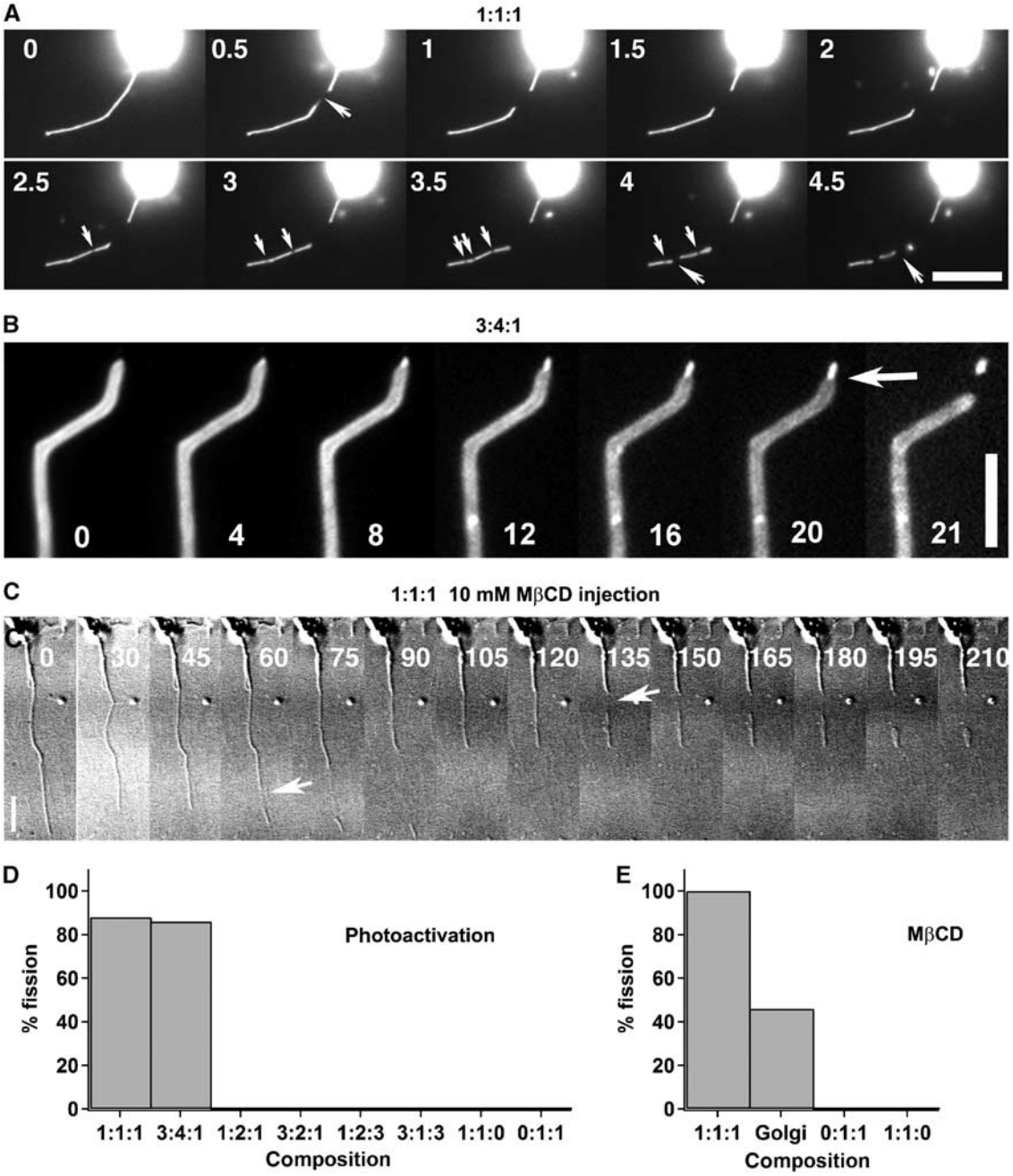


**Figure 5** Phase separation induces tube fission. (**A**) Strong photoactivation of tubes growing from 1:1:1 vesicles leads to tube fission. Fission events (large arrows) occurred predominantly at the sites of formation of weakly fluorescent domains resulting from phase separation (small arrows) (see also movie Figure 4A and movie S1 in Supplementary data). Numbers in the images A, B and C correspond to time in seconds. Bar, 10 μm. (**B**) Strong photoactivation of a tube grown from a 3:4:1 vesicle led to phase separation, resulting in a thin highly fluorescent ($L_d$ phase) tube at the tip connected to a wider and less fluorescent ($L_o$ phase) tube. A fission event occurs (arrow) after several seconds at the limit between $L_d$ and $L_o$ domains. Bar, 10 μm. (**C**) The addition of 10 mM MβCD after tube extraction leads to fission of tubes (arrows) growing from 1:1:1 vesicles (see also movie Figure 4C in Supplementary data). Time 0 corresponds to the injection of MβCD. Bars, 10 μm. (**D**) Percentages of tube networks showing at least one fission event under strong photoactivation as a function of their composition. (**E**) Percentage of networks grown from vesicles of various compositions and from Golgi membranes showing at least one fission event after injection of MβCD.

 

5A and B). With the 3:4:1 composition, more than 90% of the fission events occurred exactly at the boundary between $L_o$ and $L_d$ domains (Figure 5B, arrow). With the 1:1:1 composition, the precise position where fission occurs was difficult to determine due to the small size and the low fluorescence of the $L_o$ domains in this case (movie 5A, Supplementary data). Over 80% of the networks grown from 1:1:1 and 3:4:1 vesicles showed at least one fission event (Figure 5D). In Figure 5A, we can observe three fission events. The last two can be clearly related to phase separation (movie Figure 5A, Supplementary data). Figure 5B is particularly illuminating. At 4 s after photoactivation, a small domain of $L_d$ phase appeared at the tip of the tube. It is characterized both by an intense fluorescence and a tube diameter smaller than that of the initial tube. About 20 s later, the tube broke at the limit between the strongly and the weakly fluorescent domains. This led to the formation of an almost spherical vesicle. In some cases, the fission process led to complete fragmentation of the tubes into vesicles (movie S1, Supplementary data). The time required for tube fission after domain formation was observed to rank statistically between less than 100 ms and more than 10 s depending on lipid composition. These observations are consistent with a theoretical analysis in which rupture originates both from line tension at the domain interfaces and Gaussian curvature discontinuity (Allain *et al*, 2004).

No fission events were observed for tubes where photoactivation did not induce the formation of domains in the tubes (0:1:1, 1:1:0, 1:2:3, 1:2:1, 3:1:3 or 3:2:1—for the first four concentrations, vesicles were homogeneous, and for the last two, domains existed in the vesicles but not in the tubes) (Figure 5D). The above data thus reveal a direct link between phase separation along membrane tubes and fission. Note that this phase separation involves two liquid phases since the shape of the domains on vesicles was circular (Supplementary Figure S1A).

In good agreement with the photoactivation experiments, tube fission events were also observed after injection of MβCD. Figure 5C illustrates an experiment showing that the addition of MβCD to tubes grown out of homogeneous 1:1:1 GUVs induced two fission events (see movie Figure 5C). No fission events were observed when MβCD was added to tubes growing from vesicles remaining homogeneous (0:1:1 and 1:1:0) (Figure 5E).

A tentative hypothesis is that this is also true for biological membranes. In order to test this idea, we generated tube networks by binding kinesins to biotinylated Golgi membranes (Roux *et al*, 2002). Under control conditions, no obvious fission events could be observed. The addition of MβCD induced fission in a significant proportion of networks (Figure 5E). It is likely, as observed for model membranes, that the decrease in Chol favors phase separation of lipids present in Golgi-derived membrane tubes, and leads to their fission. This strongly supports the relevance of our *in vitro* experiments to biological systems.

A similar link between phase separation and budding has already been established experimentally (Dobereiner *et al*, 1993; Baumgart *et al*, 2003) and discussed theoretically (Julicher and Lipowsky, 1993; Chen *et al*, 1997). Our experiments confirm and extend these findings. Indeed, the tension values in our experiments are such that no budding is observed on vesicles, whereas tube fission is obtained. This is an important difference between the two experimental situations: tension prevents fission of buds in vesicles but promotes tube fission. As in the vesicle case, line tension between two coexisting phases promotes tube breakage (Allain *et al*, 2004) but tension enhances the effect by reducing the tube diameter.

It is a characteristic of many systems in biology to work in the vicinity of a phase transition in order to increase their sensitivity (Duke and Bray, 1999; Camalet *et al*, 2000; Eguiluz *et al*, 2000). Such proximity was speculated early for membranes, but without reference to intracellular transport (Overath *et al*, 1970; Wisnieski *et al*, 1974; Bloom *et al*, 1991). Our results suggest a clear biological function: one of the main roles of the numerous proteins implicated in sorting and fission events (Slepnev and De Camilli, 2000) could then be to trigger phase separation of membrane lipids, either by clustering specific lipids or by inducing membrane tubulation. Proteins (e.g. dynamin) might locally change the lipid composition in order to induce a phase separation that will promote the local fission of the membrane.

## Materials and methods

### *Reagents*

Lipids (BSM, DOPC, Chol and *N*-Cap-biotinyl-dioleyl-phosphoethanolamine (Biot-Cap-DOPE)) and brain ovine GM1 (asialo-GM1-ganglioside) were purchased from Avanti Polar Lipids. $BODIPY_{FL}$-$C_5$-hexadecanoyl phosphatidylcholine, NBD-$C_5$-hexadecanoyl phosphatidylcholine and *N*-(6-tetramethylrhodaminethiocarbamoyl)-1,2-dihexadecanoyl-*sn*-glycero-3-phosphoethanolamine (TRITC-DHPE) were obtained from Molecular Probes. All chemicals were purchased from Sigma Aldrich, except ATP and GTP, which were obtained from Roche Molecular Biochemicals. Streptavidin beads (100 nm) were purchased from Bangs Laboratories (Carmel, IN). Biotinylated hemagglutinin-kinesin (a gift of F Nédélec, EMBL, Heidelberg) was purified as described previously (Surrey *et al*, 1998). Cholera toxin was obtained from Sigma and labeled using the Cy3-labeling kit from Amersham.

### *Giant unilamellar vesicles*

GUVs were grown using the electroformation technique (Angelova *et al*, 1992) at 50°C, over the melting temperature of SM. To make lipid mixtures, BSM (average MW 731 g) and DOPC (MW 785 g) were considered to have the same molecular weight and Chol (MW 386 g) half of it. As the incorporation of 1% GM1 led to segregation of 1:1:1 vesicles, 3% Chol had to be added to restore fluorescence homogeneity. GM1 localization was detected by adding 3 μg/ml Cy3-cholera toxin to the mixture, which binds to GM1.

### *Phase separation induced by photoactivation*

Two illumination conditions were used: fast phase separation was obtained using an HBO 100 W mercury lamp mounted on a Zeiss Axiovert 200 microscope, on vesicles containing only 0.5% of the $BODIPY_{FL}$-$C_5$-HPC probe. The lamp was used at 50% of its maximal intensity with an excitation filter at 525 nm, generating a light intensity of 3.5 mW (exit of the objective × 100 (numerical aperture (NA) 1.4, Plan Apochromat, Zeiss)), and 100 images were acquired using a $CoolSNAP^{HQ}$ camera (Princeton Instruments), 100 ms each, leading to 10 s of intense photoactivation. Under these conditions, phase separation occurred within a second and led to fission of tubes after several seconds (strong photoactivation). Under the 3D fast microscope, a low light intensity (10 μW, exit of the objective) at GFP excitation wavelength (510 nm) and 1% of fluorescent marker (because 0.5% did not lead to phase separation, as less oxidized Chol was generated under these illumination conditions) allowed phase separation to occur within 10 s (weak photoactivation).

### *Thin-layer chromatography analysis*

A 1 mg portion of 1:1:1 BSM-Chol-DOPC containing 1% of $BODIPY_{FL}$-$C_5$-HPC was resuspended in 0.5 ml of water by vortexing for several minutes. Small unilamellar vesicles (SUVs) were formed

by continuous sonication for 3–4 min. SUVs were then photo-activated by placing the eppendorf tube in a laser beam (250, 25 or 0.6 mW) at 514 nm for 2 h. The intensity of the laser used in Supplementary Figure S2A was 250 mW (maximum). The suspension was dried in a speedvac after transfer to a glass tube, and traces of water were removed by placing the tube overnight in a vacuum chamber. Then, lipids were resuspended in $CHCl_3$, and analyzed on TLC silica plates (WHATMAN AL SIL G/UV, cat no. 4420222). To separate properly different sterols, a mixture of 95% chloroform and 5% acetone was used. With this eluent, glycerolipids and sphingolipids do not migrate. Sterols were revealed by 10% phosphotungstic acid in 90% ethanol and heating the plate at 90°C in an oven for 15 min. Quantities could not be accurately measured with this chemical reaction, but about twice less oxidized Chol was found at 25 mW than at 250 mW, and more then 10 times less at 0.6 mW.

#### *3D fast microscopy*

A setup developed at the Curie Institute was used and has been previously described by Savino *et al* (2001). It consisted of a Leica DM RXA microscope equipped with a piezoelectric translator (PI-FOC; Physik Instrumente, Waldbron, Germany) placed at the base of a ×100 Plan Apochromat (NA 1.4; Leica). No deconvolution process was used. For each tube network, six stacks of 80–100 images were acquired every 15 s, each image being taken every 0.3 μm by a CoolSNAP$^{HQ}$ camera (Princeton Instruments). Each image was acquired for 50–70 ms.

#### *Measurement of bending rigidity*

The force $f$ required to pull a homogeneous tube depends on the bending rigidity $\kappa$ and the tension $\sigma$ of the membrane: $f = 2\pi\sqrt{2\kappa\sigma}$. Thus, the bending rigidity can be deduced directly from the force measurement during the tube extension, with a fixed membrane tension. This was achieved by combining an optical tweezers setup with a micropipette technique.

Light from a solid-state, diode-pumped Nd:YAG laser (1064 nm, 2.5 W, continuous wave, Coherent) was focused, using a ×100/1.3 NA oil immersion objective (Axiovert 200; Zeiss), to construct a single-beam optical trap. The $X$–$Y$–$Z$ position of the trapping zone in the microscope was controlled by means of external optics. Video images of the captured beads (streptavidin polystyrene particles, radius $R = 1.76$ μm) were recorded and analyzed off-line using a custom-made tracking software (provided by Konstantin Zeldovitch, Curie Institute) with a temporal resolution of 40 ms and a subpixel spatial resolution of 35 nm. The trapping stiffness, $\kappa_f$, was calibrated by measuring the fluctuations of a captured bead for incident laser powers lower than 200 mW ($\kappa_f = k_B T/\langle \Delta x^2 \rangle$) and against Stokes' drag force for laser powers higher than 200 mW ($\kappa_f \Delta x = 6\pi\eta R v$, where $\Delta x$ is the displacement of the bead in the trap, $\eta$ is the water viscosity and $v$ is the velocity of the moving chamber). From these two methods, the stiffness of the tweezers was found to be of the order of $0.12 \pm 0.01$ pN/nm/W.

The micropipette technique is classically used (Evans and Rawicz, 1990) for fixing the tension in a GUV. A micropipette of typically 4 μm diameter at the tip is connected to a mobile water reservoir on one end, and aspirates the GUV on the other. The hydrostatic pressure $\Delta P$ fixes the membrane tension; it is controlled by the vertical position of the water reservoir. In fact, using Laplace's law, it can easily be shown that

$$\sigma = \frac{\Delta P . R_{pip}}{2(1 - R_{pip}/R_{ves})}$$

where $R_{pip}$ is the pipette radius and $R_{ves}$ the vesicle radius (Evans and Rawicz, 1990). This micropipette can be moved in $X$ and $Z$ directions by micrometric displacements and in the $Y$ direction parallel to the pipette axis by a piezoelectric stage (Physik Instrumente, Waldbron, Germany).

To insure adhesion to a 3.5 μm streptavidin-coated bead, 0.005% (n/n) DOPE-PEG2000-biotin was added to the lipid mixture. The GUV held by the micropipette was pressed against the bead for about 1 s, and then retracted at 0.2 μm/s. The bead position was simultaneously recorded.

#### *Assay for tube formation*

Membrane tubes were pulled out of GUVs and Golgi membranes as previously described (Roux *et al*, 2002). Briefly, biotinylated kinesins were bound to biotinylated lipids incorporated in membrane via nonfluorescent 100 nm streptavidin beads. Kinesin-coated beads and GUVs were sequentially injected in a 25 μl observation chamber coated with taxol-polymerized microtubules and containing 1 mM ATP. All the experiments were performed at room temperature, typically 22°C. Enriched rat liver Golgi membranes were purified according to standard procedure (Slusarewicz *et al*, 1994). Tubes were observed either by video enhanced differential interference contrast (VE-DIC) or by fluorescence microscopy (Roux *et al*, 2002).

#### *Fluorescence intensity measurement*

For each network, two 12-bit images were acquired at two different $Z$ positions using confocal microscopy. Tube and vesicle images were acquired at the substrate and equatorial plane of the vesicle, respectively (see Figure 3A). The quantitative analysis was performed using ImageJ freeware (http://rsb.info.nih.gov/ij). The tube and the vesicle intensities were deduced from the maximum intensity of a rectangular section perpendicular to the tube axis in the tube image and perpendicular to the membrane in the vesicle image, respectively. $I_G^t$ and $I_G^v$ represent the intensities in the tubes and in the vesicles of the fluorescent complex GM1/Cy3-cholera toxin, respectively. Similarly, $I_B^t$ and $I_B^v$ are the intensities in the tubes and vesicles of BODIPY$_{FL}$-C$_5$-HPC, respectively. The fluorescence ratio $FR = (I_B^t/I_G^t)/(I_B^v/I_G^v)$ was calculated for each network. Values superior to 1 correspond to a relative enrichment in the tube of BODIPY$_{FL}$-C$_5$-HPC, whereas values inferior to 1 would correspond to enrichment of the GM1/Cy3-cholera toxin complex. No relative sorting of the fluorophores corresponds to a value of 1.

#### *Supplementary data*

Supplementary data are available at *The EMBO Journal* Online.

## Acknowledgements

We thank the microscopy platform team of the Curie Institute, J-B Sibarita, V Fraisier, J de Mey and J Salamero, for their valuable technical support. We thank J-F Joanny and I Dérényi for illuminating discussions. We also thank B Antonny, J-B Manneville, O Owar, F Perez and K Simons for critical reading. We acknowledge G van Meer and L Bagatolli for input to this work. We thank J Plastino for corrections of this manuscript. This work was supported by CNRS grants (ACI 'Dynamique et réactivité des assemblages biologiques' and ACI 'Nanosciences et nanotechnologies') and the Curie Institute (PIC 'La Physique à l'Echelle de la Cellule').

## References

Allain J-M, Storm C, Roux A, Ben Amar M, Joanny JF (2004) Fission of a multiphase membrane tube. *Phys Rev Lett* **93:** 158104

Angelova MI, Soléau S, Méléard P, Faucon JF, Bothorel P (1992) Preparation of giant vesicles by external AC electric fields. Kinetics and applications. *Prog Colloid Polym Sci* **89:** 127–131

Baumgart T, Hess ST, Webb WW (2003) Imaging coexisting fluid domains in biomembrane models coupling curvature and line tension. *Nature* **425:** 821–824

Bloom M, Evans E, Mouritsen OG (1991) Physical properties of the fluid lipid-bilayer component of cell membranes: a perspective. *Q Rev Biophys* **24:** 293–397

Brugger B, Sandhoff R, Wegehingel S, Gorgas K, Malsam J, Helms JB, Lehmann WD, Nickel W, Wieland FT (2000) Evidence for segregation of sphingomyelin and cholesterol during formation of COPI-coated vesicles. *J Cell Biol* **151:** 507–518

Camalet S, Duke T, Jülicher F, Prost J (2000) Auditory sensitivity provided by self-tuned critical oscillations of hair cells. *Proc Natl Acad Sci USA* **97:** 3183–3187

 

Chen C-M, Higgs PG, Mackintosh FC (1997) Theory of fission for two-component lipid vesicles. *Phys Rev Lett* **79:** 1579–1582

de Almeida RF, Fedorov A, Prieto M (2003) Sphingomyelin/phosphatidylcholine/cholesterol phase diagram: boundaries and composition of lipid rafts. *Biophys J* **85:** 2406–2416

Derenyi I, Julicher F, Prost J (2002) Formation and interaction of membrane tubes. *Phys Rev Lett* **88:** 238101

Derenyi I, Julicher F, Prost J (2004) Formation and dynamics of membrane tubes. *22nd International Conference on Statistical Physics*, (http://www.physics.iisc.ernet.in/~statphys22), Bangalore (India)

Dietrich C, Bagatolli LA, Volovyk ZN, Thompson NL, Levi M, Jacobson K, Gratton E (2001) Lipid rafts reconstituted in model membranes. *Biophys J* **80:** 1417–1428

Dobereiner HG, Kas J, Noppl D, Sprenger I, Sackmann E (1993) Budding and fission of vesicles. *Biophys J* **65:** 1396–1403

Duke TA, Bray D (1999) Heightened sensitivity of a lattice of membrane receptors. *Proc Natl Acad Sci USA* **96:** 10104–10108

Edidin M (2003) The state of lipid rafts: from model membranes to cells. *Annu Rev Biophys Biomol Struct* **32:** 257–283

Eguiluz VM, Ospeck M, Choe Y, Hudspeth AJ, Magnasco MO (2000) Essential nonlinearities in hearing. *Phys Rev Lett* **84:** 5232–5235

Evans E, Rawicz W (1990) Entropy-driven tension and bending elasticity in condensed-fluid membranes. *Phys Rev Lett* **64:** 2094–2097

Huttner WB, Schmidt A (2000) Lipids, lipid modification and lipid–protein interaction in membrane budding and fission—insights from the roles of endophilin A1 and synaptophysin in synaptic vesicle endocytosis. *Curr Opin Neurobiol* **10:** 543–551

Julicher F, Lipowsky R (1993) Domain-induced budding of vesicles. *Phys Rev Lett* **70:** 2964–2967

Kahya N, Scherfeld D, Bacia K, Poolman B, Schwille P (2003) Probing lipid mobility of raft-exhibiting model membranes by fluorescence correlation spectroscopy. *J Biol Chem* **278:** 28109–28115

Kilsdonk EP, Yancey PG, Stoudt GW, Bangerter FW, Johnson WJ, Phillips MC, Rothblat GH (1995) Cellular cholesterol efflux mediated by cyclodextrins. *J Biol Chem* **270:** 17250–17256

Lawrence JC, Saslowsky DE, Edwardson JM, Henderson RM (2003) Real-time analysis of the effects of cholesterol on lipid raft behavior using atomic force microscopy. *Biophys J* **84:** 1827–1832

Leibler S, Andelman D (1987) Ordered and curved meso-structures in membranes and amphiphilic films. *J Phys* **48:** 2013–2018

Mukherjee S, Maxfield FR (2000) Role of membrane organization and membrane domains in endocytic lipid trafficking. *Traffic* **1:** 203–211

Mukherjee S, Soe TT, Maxfield FR (1999) Endocytic sorting of lipid analogues differing solely in the chemistry of their hydrophobic tails. *J Cell Biol* **144:** 1271–1284

Overath P, Schairer HU, Stoffel W (1970) Correlation of *in vivo* and *in vitro* phase transitions of membrane lipids in *Escherichia coli*. *Proc Natl Acad Sci USA* **67:** 606–612

Roux A, Cappello G, Cartaud J, Prost J, Goud B, Bassereau P (2002) A minimal system allowing tubulation with molecular motors pulling on giant liposomes. *Proc Natl Acad Sci USA* **99:** 5394–5399

Savino TM, Gebrane-Younes J, De Mey J, Sibarita JB, Hernandez-Verdun D (2001) Nucleolar assembly of the rRNA processing machinery in living cells. *J Cell Biol* **153:** 1097–1110

Schmidt A, Wolde M, Thiele C, Fest W, Kratzin H, Podtelejnikov AV, Witke W, Huttner WB, Soling HD (1999) Endophilin I mediates synaptic vesicle formation by transfer of arachidonate to lysophosphatidic acid. *Nature* **401:** 133–141

Seifert U (1993) Curvature-induced lateral phase segregation in two-component vesicles. *Phys Rev Lett* **70:** 1335–1338

Slepnev VI, De Camilli P (2000) Accessory factors in clathrin-dependent synaptic vesicle endocytosis. *Nat Rev Neurosci* **1:** 161–172

Slusarewicz P, Hui N, Warren G (1994) Purification of rat liver Golgi stacks. In *Cell Biology: A Laboratory Handbook*, Celis JE (ed) Vol. 1, pp 509–516. San Diego, CA: Academic Press

Surrey T, Elowitz MB, Wolf PE, Yang F, Nedelec F, Shokat K, Leibler S (1998) Chromophore-assisted light inactivation and self-organization of microtubules and motors. *Proc Natl Acad Sci USA* **95:** 4293–4298

Svetina S, Zeks B, Waugh RE, Raphael RM (1998) Theoretical analysis of the effect of the transbilayer movement of phospholipid molecules on the dynamic behavior of a microtube pulled out of an aspirated vesicle. *Eur Biophys J* **27:** 197–209

van Meer G, Lisman Q (2002) Sphingolipid transport: rafts and translocators. *J Biol Chem* **277:** 25855–25858

Veatch SL, Keller SL (2002) Organization in lipid membranes containing cholesterol. *Phys Rev Lett* **89:** 268101

Veatch SL, Keller SL (2003) A closer look at the canonical 'raft mixture' in model membrane studies. *Biophys J* **84:** 725–726

Wisnieski BJ, Parkes JG, Huang YO, Fox CF (1974) Physical and physiological evidence for two phase transitions in cytoplasmic membranes of animal cells. *Proc Natl Acad Sci USA* **71:** 4381–4385